

Holographic QCD in the Veneziano limit.

Ioannis Iatrakis^α

^αUniversity of Utrecht
Heraklion Workshop on Theoretical Physics

September 6, 2016

Outline

1 Introduction

- Motivation

2 QCD in the Veneziano limit

3 Holographic V-QCD

- The bulk fields & the dual operators.
- The action
- Constraining the potentials
- The ground state
- The fluctuations at $T = 0$.
- QCD string collectivization
- Finite chemical potential
- CP-odd sector of V-QCD
- Inverse Magnetic Catalysis in Holographic QCD

4 Conclusions & Outlook

Motivation

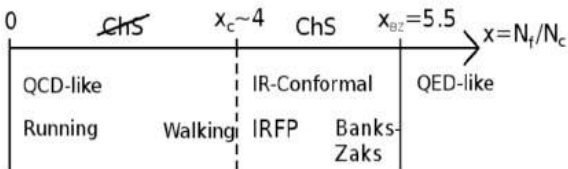
- We are interested in describing strongly coupled phenomena of QCD.
- Much of the effort is focused on the probe approximation $N_f \ll N_c$.
- We review a holographic model of QCD in the Veneziano limit where $N_f \sim N_c$.
- We firstly introduce the glue part of the action (IHQCD).
- We then add the flavor degrees of freedom via tachyon-DBI action.
- Those two parts are eventually fused.
- The topics which will be presented then include:
 - The ground state and the spectrum of the model at $T = 0$ and $T \neq 0$.
 - The radial flow puzzle in Heavy Ion Collisions.
 - The CP-odd dynamics and the $U(1)_A$ anomaly.
 - Inverse magnetic catalysis in V-QCD.

V-QCD

Veneziano introduced the limit where

$$N_c \rightarrow \infty, \quad N_f \rightarrow \infty, \quad x = \frac{N_f}{N_c} \rightarrow \text{fixed}, \quad \lambda = g_{YM}^2 N_c \rightarrow \text{fixed}$$

in order for the flavor to be as important as the colour in the large N_c limit. The phase diagram of the theory in terms of x is





IR

- Since the tachyon potential falls fast enough in the IR the flavor dynamics decouple from the glue.
- The criteria for a "good" IR singularity, confinement and asymptotic linear Regge trajectories of the glueball spectra fix the IR behavior of $V_g(\lambda)$

$$V_g(\lambda) \propto \lambda^{\frac{4}{3}} \sqrt{\log \lambda}.$$

- In case of, non-critical string theory in flat-background the powers are

$$\begin{aligned} \kappa(\lambda) &\sim \lambda^{-\frac{4}{3}}, & a(\lambda) &\sim \lambda^0, \\ w(\lambda) &\sim \lambda^{-\frac{4}{3}}, & V_{f0}(\lambda) &\sim \lambda^{\frac{7}{3}}, \end{aligned} \quad (\lambda \rightarrow \infty).$$

- The functions $\kappa(\lambda)$ and $w(\lambda)$ are also constrained by requiring that all the fluctuation towers have the same asymptotic Regge trajectories (including the slope).



The potentials

- A simple choice of potentials is made such that they have the appropriate UV and IR asymptotics.
- Two types of potentials (I & II) have mostly been used in the studies of V-QCD.
- The difference of **Potentials I & II** is the different choice of $a(\lambda)$, which appears in $V_f(\lambda, \tau) = V_{f0}(\lambda)e^{-a(\lambda)\tau^2}$.
- **Potentials I** : $a(\lambda) = a_0$.
- **Potentials II** : $a(\lambda) = a_0 \frac{1 + a_1 \lambda + \frac{\lambda^2}{\lambda_0^2}}{\left(1 + \frac{\lambda}{\lambda_0}\right)^{4/3}}$.

The IR fixed point

- The full dilaton potential at $\tau = 0$, namely

$$V_{\text{eff}}(\lambda) = V_g(\lambda) - xV_f(\lambda, \tau = 0),$$

must have a nontrivial IR extremum at $\lambda = \lambda_*(x)$ that moves from $\lambda_* = 0$ at $x = 11/2$ to large values as x is lowered.

- By expanding the DBI action we obtain the IR tachyon mass at the fixed point.

$$\Delta_{ir}(4 - \Delta_{ir}) = -m_{\text{IR}}^2 \ell_{\text{IR}}^2 = \frac{24a(\lambda_*)}{\kappa(\lambda_*)V_{\text{eff}}(\lambda_*)} \leq 4.$$

(Jarvinen-Kiritsis)



The vacuum solutions for $m_q = 0$

- When $x_c \leq x < 11/2$, chiral symmetry is intact. There is a unique vacuum solution with vanishing tachyon.
- When $0 < x < x_c$, chiral symmetry is broken. The dominant vacuum therefore has nonzero tachyon even though the quark mass is zero.
- For $0 < x < x_c$, there are also oscillatory solutions for the tachyon (Efimov vacua) characterized by the number of "zeros" of the tachyon.

The vacuum solutions for $m_q = 0$

- The dominant vacuum has a monotonic tachyon profile with diverging IR asymptotics.
- The oscillating tachyon vacua are unstable.

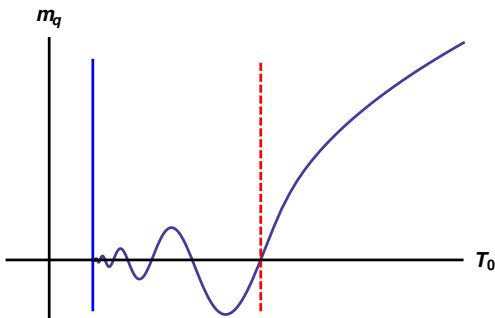


Figure: The quark mass in terms of the parameter T_0 that controls the tachyon's IR asymptotics. For example, $\tau_{ir}(r) \simeq T_0 e^{Cr}$.

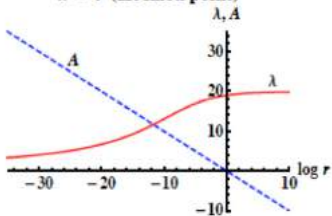


The ground state

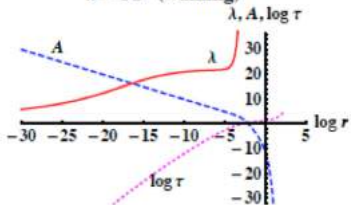


The dominant $T = 0$ vacuum solutions for Potentials I, $x_c = 3.9956$.

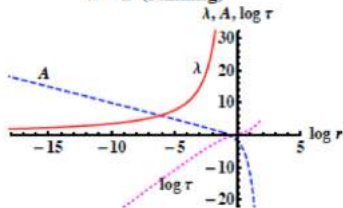
$x = 4$ (IR fixed point)



$x = 3.9$ (walking)



$x = 2$ (running)



Quadratic fluctuations

We separate the fluctuations into two classes: the non-singlets and singlets under the flavor group, (Arañzabal-Jarvinen-Kiritsis). The non-singlets include:

- the left and right gauge fields which combine to the vector and axial vector combinations (1^{--} , 1^{++} states)

$$V_M = \frac{A_M^L + A_M^R}{2}, \quad A_M = \frac{A_M^L - A_M^R}{2}.$$

- the pseudoscalars which come from the longitudinal part of the axial-vector and the phase of the tachyon (0^{-+} states).
- the scalars which come from the tachyon modulus (0^{++} states).

Quadratic fluctuations

The singlet fluctuations include:

- a rank 2 traceless symmetric tensor, coming from the metric, which corresponds to the 2^{++} glueballs,
- two scalar which are gauge invariant combinations of the fluctuations of the tachyon modulus, the metric and the dilaton. Those correspond to 0^{++} glueball which mixes with the flavor-singlet σ meson at finite x .
- two pseudoscalar gauge invariant fluctuations of the axion, the tachyon phase and the longitudinal part of the flavor-singlet axial-vector field. Those correspond to (0^{-+}) glueball which mixes with the η' meson.

The fluctuations at $T = 0$.

Non-Singlet mesons

All quantities in the model with non-zero mass dimension follow Miransky scaling in the vicinity of x_c

$$m_n \sim \Lambda_{UV} \exp\left(-\frac{\kappa}{\sqrt{x_c - x}}\right).$$

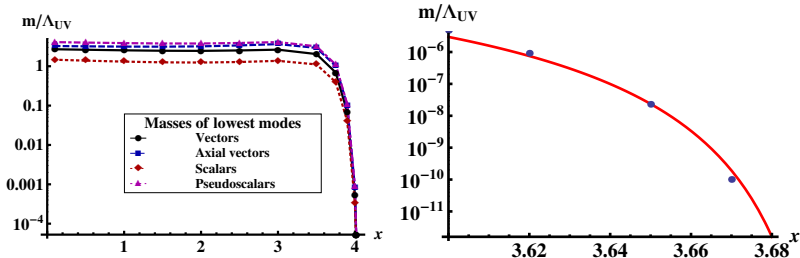


Figure: The lowest nonzero masses of all four towers of non-singlet mesons, as a function of x , in units of Λ_{UV} , below the conformal window. Left: Potentials I, with $x_c \simeq 4.0830$. Right: A fit of the ρ mass to the Miransky scaling factor, for Potentials II, with $x_c \simeq 3.7001$.

The singlet mesons

Is there a Goldstone mode (dilaton), due to the breaking of conformal invariance at $x = x_c$?

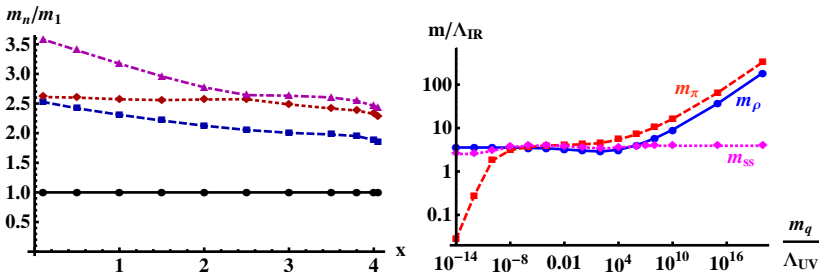


Figure: Left: The ratios of the singlet scalar masses of up to the fourth massive states as a function of x for potentials I at $m_q = 0$. Right: The pion, ρ and the lowest singlet scalar state as a function of the quark mass for $x \rightarrow x_c$. The pion follows the Gell-Mann-Oakes-Renner relation as $m_q \rightarrow 0$ and it becomes the heaviest for large m_q , (Jarvinen).

Heavy-Ion collisions

- Radial flow puzzle addresses the fact the central pA collisions have large rapidity of the radial flow

$$y_{\perp}^{AA,peripheral} < y_{\perp}^{AA,central} < y_{\perp}^{pA,central} \sim y_{\perp}^{pp,highest},$$

while the initial densities are

$$\frac{dN_{central}^{pA}}{dA_{\perp}} \sim \frac{dN_{peripheral}^{AA}}{dA_{\perp}} < \frac{dN_{central}^{AA}}{dA_{\perp}} < \frac{dN_{highest}^{pp}}{dA_{\perp}}.$$

- It was recently proposed that in maximal multiplicity pA collisions there is a QCD string system which collapses, collectivizes and forms the QGP which then explodes (II-Kalaydzhyan-Ramamurti-Shuryak).
- When the string system collectivizes chiral symmetry is locally restored as a result of the string interaction and the Quark Gluon Plasma is formed.



Strings and Gauge/Gravity duality

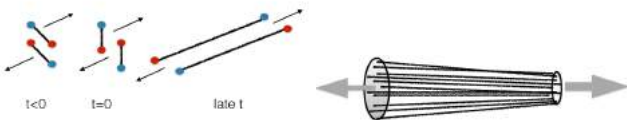


Figure: (a) Two-string production resulting from color reconnection. (b) A multi-string state, produced in pA collisions or very peripheral AA collisions, known as "spaghetti" of strings.

- The QCD string breaks $\tau_{br.} \sim 1.5 fm$ after it's production. Then, it has length $\sim 2 fm$ and radius $\sim 0.15 fm$. Hence, they can be practically considered as long straight strings.
- The QCD strings have a gluonic core and a mesonic cloud surrounding them.
- They interact through the mediation of σ mesons. Hence, we need a model where the flavor degrees of freedom are not suppressed.

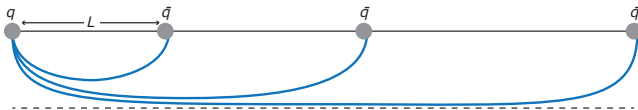


Figure: Configurations with a turning point signal area law behavior of the Wilson Loop.

- The Wilson loop of a heavy $q - \bar{q}$ pair is computed holographically by calculating the on-shell Nambu-Gotto action of a classical string with its endpoints attached on the boundary at distance L and the rest of it extending in the bulk.
- String dynamics are governed by the Nambu-Goto action

$$S_{NG} = -T_f \int d\tau d\sigma \sqrt{-\det g_s} , \quad (g_s)_{\alpha\beta} = (g_s)_{\mu\nu} \partial_\alpha X^\mu \partial_\beta X^\nu ,$$

where we use the string frame metric

$$(g_s)_{\mu\nu} = e^{2A_s(z)} \eta_{\mu\nu} , \quad A_s(z) = A(z) + \frac{2}{3} \Phi(z) .$$

V-QCD exhibits confinement in the sense that the holographic computation of Wilson loop produces an area law.

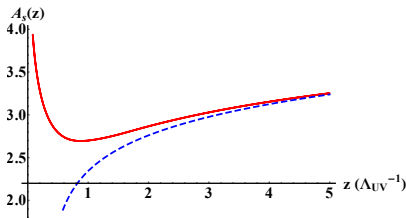


Figure: The combination $A_s(z)$ as a function of the holographic coordinate z (solid) compared to its IR (large z) asymptotics (dashed). $A_s(z)$ has a minimum corresponding to the equilibrium scale of the QCD string.

The string equilibrates at the point $A'_s(z_*) = 0$.



- The scalar fluctuations of the model describe the mixed scalar glueballs and mesons, Fig. 6. The relevant excitations of the tachyon, dilaton, and the scalar part of the metric.
- Selecting the numerical value of Λ_{UV} from the second and third state masses, which are narrow and therefore well mapped to phenomenology, we fix the absolute units in our model to be

$$\Lambda_{UV} = 387 \text{ MeV}, \quad m_\sigma = 592 \text{ MeV}.$$

- Then, of the masses of the higher states read

$$m_2 = 1370 \text{ MeV}, \quad m_3 = 1525 \text{ MeV},$$

$$m_4 = 1881 \text{ MeV}, \quad m_5 = 2019 \text{ MeV}.$$

- Hence, the lightest σ meson state is followed by the two mixed meson and glueball states $f_0(1370)$ and $f_0(1500)$.

The coupled system of equations for the spectrum reads

$$\begin{pmatrix} H_{\zeta}^{(0)} & V_{\xi} \\ V_{\zeta} & H_{\xi}^{(0)} \end{pmatrix} \begin{pmatrix} \zeta_n \\ \xi_m \end{pmatrix} = m_n^2 \begin{pmatrix} \zeta_n \\ \xi_m \end{pmatrix}$$

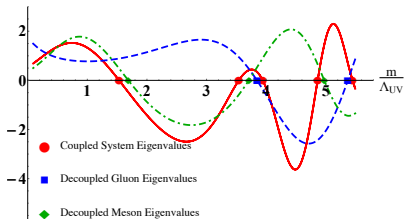
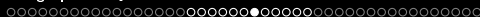


Figure: The determinant of the UV boundary value of two linearly independent solutions of the scalar fluctuation equations, versus the mass parameter in Λ_{UV} units. The solid curve's five zeros (red circles) indicate the normalizable solutions, and the corresponding masses are those of the lowest five mixed scalars. The two other curves (dashed and dot-dashed) correspond to unmixed equations.



We perform perturbation theory for the above system. The first three states in terms of the eigenstates of the uncoupled system reads

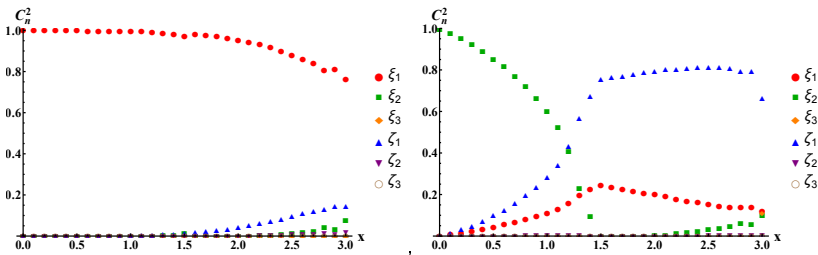


Figure: The square of the decomposition coefficients of the first two singlet scalar state in terms of the "free" eigenstates (a) lowest mixed meson state and (b) the lowest mixed glueball state.

- The string coupling vector in the basis of the free uncoupled states is $|string\rangle = (1, 1, 1, 0, 0, 0)$. It's projection to the σ state is small

$$\langle string|\sigma\rangle \simeq 0.066. \quad (1)$$

- We consider infinitely long strings, $X^M = (t, x, X_2(t), X_3(t), Z(t))$, and study the scalar excitations that they generate as classical sources.
- We expand the NG action to first order in the fluctuation of the dilaton field.
- We expand the fields and the source on the basis of the free eigenstates and solve for the fluctuation fields.
- Then, we solve the system of the scalar fluctuation equations with a source for the dilaton fluctuation.

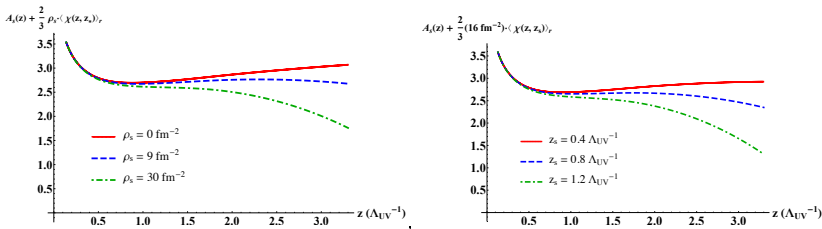


Figure: The background potential, (a) without and with string-induced fluctuations, all placed at the minimum of the z potential (z_*) with the denoted transverse density, and (b) induced by strings with density 16 fm^{-2} , all placed at various points in the z coordinate (denoted z_s). The r dependence of χ is averaged out, leaving only the density dependence of the fluctuation.

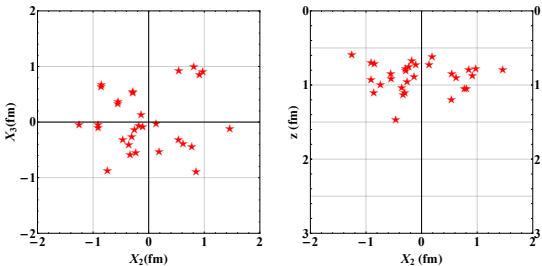


Figure: The string snapshots at $t = 1.0 \text{ fm}/c$

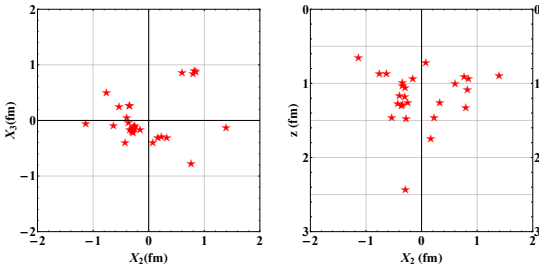
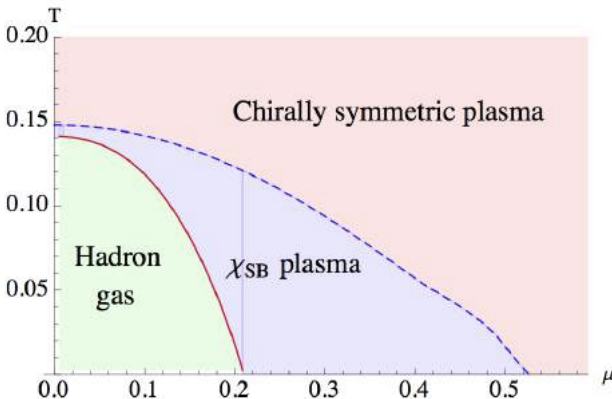


Figure: The string snapshots at the point where the first string hits the IR cut-off at $t = 1.32 fm/c$.

$T - \mu$ phase diagram, $x = 1$.

In case of a boundary QFT of finite density there is a non-trivial bulk vector field at the ground state dual to the chemical potential. It's asymptotics in the UV is of the form $V_0(r) \simeq \mu + nr^2$.





Quasinormal modes for $\mu = 0$

- The quasinormal modes of the vector and axial vector states for $\mathbf{k} = 0$ are found as a function of the temperature and chemical potential for zero spatial momentum.
- $\omega_R \rightarrow 2\pi T$, for large T , similar to the screening masses found in lattice studies, (Bernard-Ogilvie-DeGrand-DeTar-Gottlieb-Krasnitz, -Sugar-Toussaint).

(Il-Zahed)

Quasinormal modes for $\mu = 0$

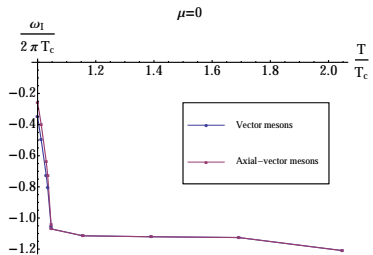
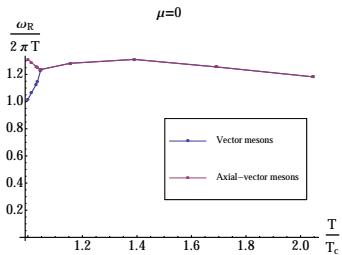


Figure: The real (left) and imaginary (right) part of the lowest quasinormal frequency of transverse vector and axial-vector mesons as a function of temperature at $\mu = 0$. T_c is the deconfinement transition temperature at $\mu = 0$.



The flavor conductivity and diffusion constant for $\mu = 0$.

- The conductivity of the flavor vector and axial-vector current is calculated by solving the fluctuation equations in the limit $\omega \rightarrow 0$.
- Studying the retarded correlator of the longitudinal vector current in the hydrodynamic regime ($\omega, k \ll T$), we found the diffusion constant ($\omega = -iD k^2$) in terms of T .

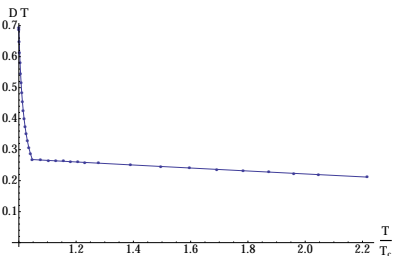
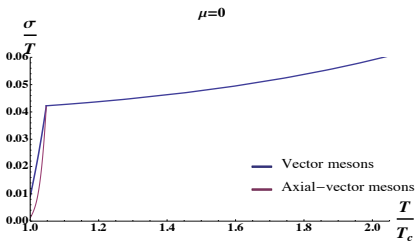


Figure: **Left:** The transport coefficients of vector and axial-vector flavor currents along the $\mu = 0$ (left) line of the phase diagram in Fig. 34. **Right:** The diffusion constant of vector flavor current in terms of T at $\mu = 0$.

The CP-odd dynamics is governed by the $U(1)_A$ anomaly

$$\partial_\mu J^{(5)\mu} = \frac{N_f}{16\pi^2} \epsilon^{\mu\nu\rho\sigma} \text{Tr} (F_{\mu\nu} F_{\rho\sigma}) + 2i m_q \bar{q} \gamma^5 q .$$

The corresponding bulk operators

Bulk Fields	Dual Operator
α	$\text{Tr} [F \wedge F]$
ξ	$\bar{q} \gamma^5 q$
A_μ	$J_\mu^{(5)} = \bar{q} \gamma_\mu \gamma^5 q$

where the vacuum tachyon ansatz is $T = \tau(r) e^{i\xi(r)} \mathbb{I}_{N_f}$. The CP-odd action is

$$S_a = -\frac{M^3 N_c^2}{2} \int d^5x \sqrt{-g} Z(\lambda) [d\mathbf{a} - x (2V_a(\lambda, \tau) A - \xi dV_a(\lambda, \tau))]^2 ,$$

in terms of the QCD axion $\mathbf{a} = \frac{\alpha}{N_c}$.

(Arañ-Il-Jarvinen-Kiritsis)

- IR regularity requires V_a to vanish faster than V_f .
- One choice is $V_a \sim e^{-a_1 \tau^2 - a_2 |\tau|}$.
- $Z(\lambda)$ is fixed by pseudoscalar glueball spectra.
- The bulk action is invariant under the bulk gauge transformation

$$A_\mu \rightarrow A_\mu + \partial_\mu \varepsilon, \quad \xi \rightarrow \xi - 2\varepsilon, \quad \mathbf{a} \rightarrow \mathbf{a} + 2x V_a \varepsilon,$$

signaling the $U(1)_A$ of the boundary theory.

- We consider background solutions with non-trivial $A(r)$, $\lambda(r)$, $\tau(r)$ and $\bar{\mathbf{a}} = \mathbf{a} + x\xi V_a$.
- $\bar{\mathbf{a}}$ is dual to the $U_A(1)$ invariant combination $\bar{\theta}/N_c = \theta/N_c + \arg(\det M_q)/N_c$.
- The free energy $\mathcal{E}(\bar{\theta})$ and the topological susceptibility

$$\chi(\bar{\theta}) = \mathcal{E}''(\bar{\theta})$$

of the ground state are calculated.

- For small quark mass

$$\bar{\mathcal{E}}(\bar{\theta}) - \bar{\mathcal{E}}(0) = -\langle \bar{q}q \rangle \Big|_{m_q=0} \left(1 - \cos \frac{\bar{\theta}}{N_f} \right) m_q + \mathcal{O}(m_q^2).$$

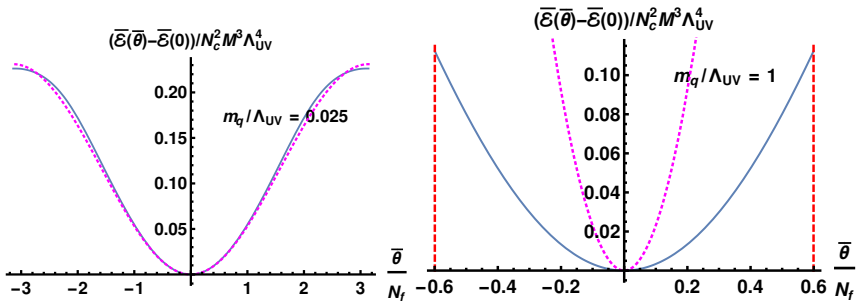


Figure: The free energy of the ground state with respect to $\bar{\theta}$ for the potentials I at $x = 2/3$ for two different values of quark mass. Blue line: full numerical result. Purple line: $m_q \rightarrow 0$ approximation.

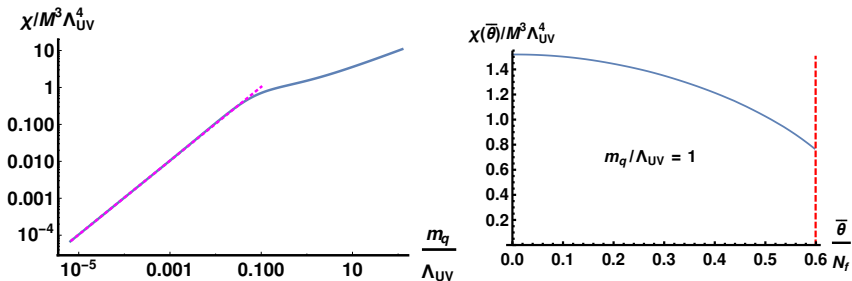


Figure: Left: The topological susceptibility as a function of the quark mass for potentials I, $x = 2/3$. Right: The generalized topological susceptibility in terms of $\bar{\theta}$.



The singlet pseudoscalar masses are computed as a function of x . In the small x and m_q limit in case of $\bar{\theta} = 0$, the Witten-Veneziano formula is verified analytically and numerically

$$m_{\eta'}^2 = m_{\pi}^2 + x \frac{N_f N_c \chi_{\text{YM}}}{f_{\pi}^2}, \quad (2)$$

where χ_{YM} is the YM topological susceptibility and f_{π}^2 is the pion decay constant.

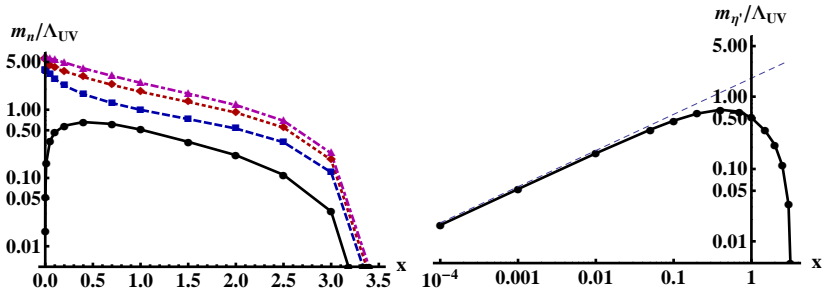


Figure: Left: The masses of the four lowest singlet pseudoscalar states as a function of x for potentials II. Right: The η' and pion mass in the limit of small x ($x = 0.0001$)



The Gell-Mann-Oakes-Renner relation for the pion mass at finite $\bar{\theta}$ is shown

$$f_{\pi,0}^2 m_\pi^2 = -\langle \bar{q}q \rangle |_{m_q=0} m_q \cos \frac{\bar{\theta}}{N_f} + \mathcal{O}(m_q^2),$$

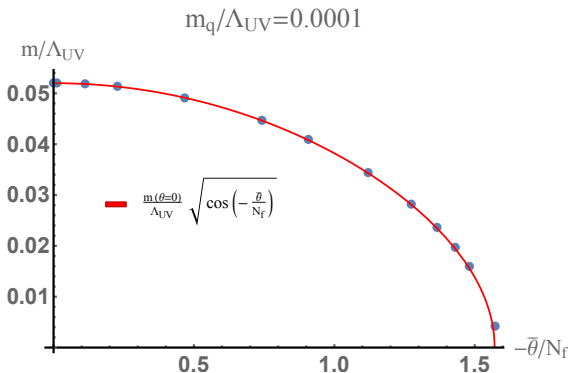


Figure: The pion mass in terms of the theta angle.

- The inverse magnetic catalysis in QCD is the phenomenon of the decatalysis of chiral symmetry breaking at large magnetic field.
- The dynamics of the model is studied in the presence of external magnetic field

$$V_\mu = (0, -x_2 B/2, x_1 B/2, 0, 0) .$$

$$ds^2 = e^{2A(r)} \left(\frac{dr^2}{f(r)} - f(r) dt^2 + dx_1^2 + dx_2^2 + e^{2W(r)} dx_3^2 \right) .$$

- The confinement-deconfinement transition, chiral transition temperature and the chiral condensate are calculated as function of the magnetic field.
- The potential $w(\lambda)$ is parameterized by

$$w(\lambda) = \frac{\sqrt{1 + \log(1 + c \lambda)}}{\left(1 + \frac{3}{4} \left(\frac{115 - 16x}{27} + \frac{1}{2}\right) c \lambda\right)^{4/3}} .$$

- Depending on the parameter c , we find different behavior of the observables in terms of the magnetic field.

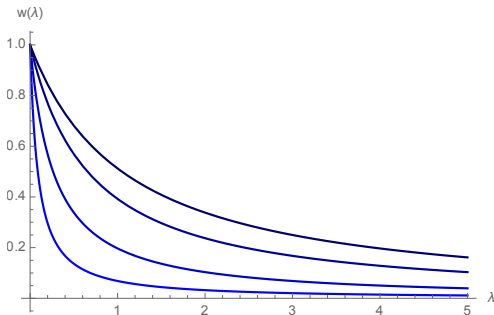


Figure: $w(\lambda)$ for different values of the parameter $c = 1$ for $x = 1$. The curves are for $c = 0.25, 0.4, 1$ and 3 . Similar values of c correspond to darker curves.

The quark condensate as a function of T and B is calculated

$$\Sigma(T, B) = \frac{1}{\langle \bar{q}q \rangle(0, 0)} (\langle \bar{q}q \rangle(T, B) - \langle \bar{q}q \rangle(0, 0)) + 1, \quad \Delta\Sigma = \Sigma(T, B) - \Sigma(T, 0).$$

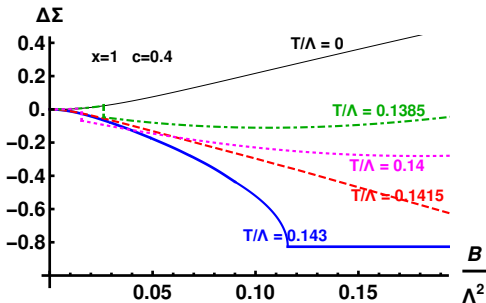


Figure: The change of the chiral condensate, $\langle \bar{q}q \rangle$, as a function of B for constant T , $c = 0.4$, zero quark mass, $m_q = 0$, and $x = 1$. The dimensionful quantities are measured in units of Λ .

Conclusions

- V-QCD matches the phase structure of the field theory at finite x .
- Below the conformal window, $x < x_c$, the spectra are discrete and gapped (except for the pions) and agree qualitatively with QCD. All masses in the walking region obey Miransky scaling. There is no light "dilaton" state. The approximate conformal symmetry is correlated with Miransky scaling instead.
- A nice qualitative picture of QCD string interactions and the collectivization of low multiplicity systems can be given in the context of V-QCD.
- The finite T and μ fluctuation analysis shows qualitative agreement with the expectations from the field theory.
- The CP-odd physics of the model give interesting results at finite θ backgrounds for large quark mass and different x .
- The model nicely incorporates inverse magnetic catalysis.



Outlook

- Global match of the model to QCD (Jarvinen).
- Time-dependent properties of QCD (i.e. transport coefficients) can be calculated using V-QCD.
- Further study of V-QCD in finite magnetic field and chemical potential.
- Consistent study of the electromagnetic sector of QCD with some sensible choices of the potentials.
- Study of glueball and meson production in high energy and small momentum transfer proton-proton interactions (II-Ramamurti-Shuryak).
- The CP-odd sector can give interesting results, particularly at the deconfined phase. Study the axial charge generation and transport due to topological fluctuations in the limit of $N_f \sim N_c$.

Thank you